university of groningen

University Medical Center Groningen

University of Groningen

Dynamic density functional theory for microphase separation kinetics of block copolymer melts

Fraaije, J. G. E. M.

Published in:
Journal of Chemical Physics

DOI:
10.1063/1.465536

IMPORTANT NOTE: You are advised to consult the publisher's version (publisher's PDF) if you wish to cite from it. Please check the document version below.

Document Version
Publisher's PDF, also known as Version of record

Publication date:
1993

Link to publication in University of Groningen/UMCG research database

Citation for published version (APA):
Fraaije, J. G. E. M. (1993). Dynamic density functional theory for microphase separation kinetics of block copolymer melts. Journal of Chemical Physics, 99(11), 9202-9212. https://doi.org/10.1063/1.465536

Copyright
Other than for strictly personal use, it is not permitted to download or to forward/distribute the text or part of it without the consent of the author(s) and/or copyright holder(s), unless the work is under an open content license (like Creative Commons).

Take-down policy
If you believe that this document breaches copyright please contact us providing details, and we will remove access to the work immediately and investigate your claim.

Downloaded from the University of Groningen/UMCG research database (Pure): http://www.rug.nl/research/portal. For technical reasons the number of authors shown on this cover page is limited to 10 maximum.

Download date: 22-05-2019

Dynamic density functional theory for microphase separation kinetics of block copolymer melts

J. G. E. M. Fraaije

Citation: The Journal of Chemical Physics **99**, 9202 (1993); doi: 10.1063/1.465536
View online: https://doi.org/10.1063/1.465536
View Table of Contents: http://aip.scitation.org/toc/jcp/99/11
Published by the American Institute of Physics

Articles you may be interested in

The dynamic mean-field density functional method and its application to the mesoscopic dynamics of quenched block copolymer melts
The Journal of Chemical Physics **106**, 4260 (1997); 10.1063/1.473129

Dynamic simulation of diblock copolymer microphase separation
The Journal of Chemical Physics **108**, 8713 (1998); 10.1063/1.476300

Fluctuation effects in the theory of microphase separation in block copolymers
The Journal of Chemical Physics **87**, 697 (1987); 10.1063/1.453566

Dissipative particle dynamics: Bridging the gap between atomistic and mesoscopic simulation
The Journal of Chemical Physics **107**, 4423 (1997); 10.1063/1.474784

On the role of hydrodynamic interactions in block copolymer microphase separation
The Journal of Chemical Physics **110**, 9739 (1999); 10.1063/1.478939

Fluctuation effects in a symmetric diblock copolymer near the order–disorder transition
The Journal of Chemical Physics **92**, 6255 (1990); 10.1063/1.458350

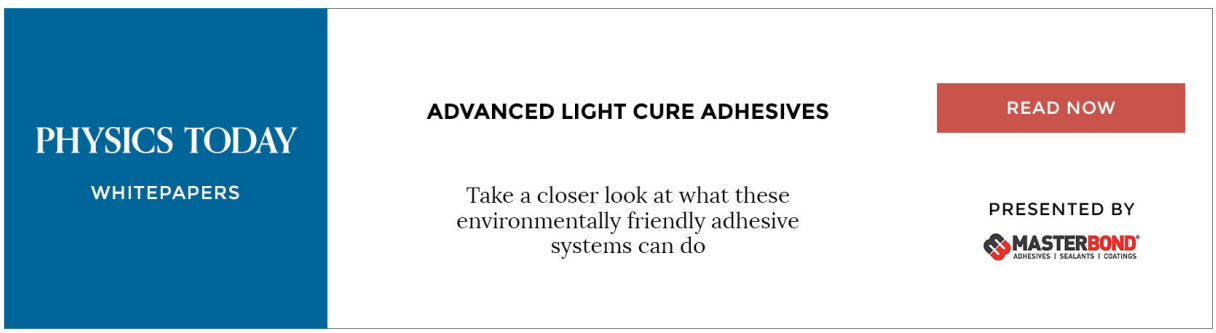

Dynamic density functional theory for microphase separation kinetics of block copolymer melts

J. G. E. M. Fraaije[a)]
Laboratory of Biophysical Chemistry, University of Groningen, Nijenborgh 4, 9747 AG Groningen, The Netherlands

(Received 20 May 1993; accepted 16 August 1993)

In this paper, we describe a numerical method for the calculation of collective diffusion relaxation mechanisms in quenched block copolymer melts. The method entails the repeated calculation of two opposing fields—an external potential field U, conjugate to the density field ρ, and an energetic interaction field E. The external field is calculated by numerical inversion of the density functionals and the energetic interaction field is calculated directly by integration over the density field. When the two fields are balanced $U=E$, we recover the self-consistent field solutions; when the two fields are off balance, the spatial gradient of $E-U$ is the thermodynamic force which drives the collective diffusion. We introduce a simple local coupling approximation for the Onsager kinetic coefficients of short freely jointed chains in weakly ordered systems. Fluctuations are added by incorporation of a random Langevin force in the diffusion equation. Numerical results of decomposition in symmetric and asymmetric diblock copolymer melts indicate that the method is capable of describing extremely slow defect annihilation relaxation modes. We find that in the nonlinear regime, the density patterns evolve to metastable states, in which isolated defects separate relatively well-ordered crystalline microdomains. These final states are typical for many industrial applications of incompletely relaxed copolymer melts.

I. INTRODUCTION

A. General

The microphase separation transitions of (block) copolymer melts have received considerable attention in the past decade. Both experimental and theoretical work (for an excellent review, see Ref. 1) has shown that these liquids may exhibit a variety of regular self-organized structures in some supercrystal lattice, such as stacked lamellas, body-centered-cubic arrays of spheres, hexagonal packed cylinders, or the fascinating ordered bicontinuous double diamond phases. So far, the attention of most studies has focused on the phase diagrams and the equilibrium density patterns. The kinetics of phase separation of copolymer melts seems a challenge for both the theoretician and the experimentalist. Remarks are made that quenching in the absence of a *biasing* field results in messy, irregular nonequilibrium states with "poorly defined morphologies" (citation from Ref. 2). Indeed, in academia, *single-crystalline* equilibrium structures are usually prepared by careful casting from solution,[3] or by a shearing technique.[2,4] These procedures can take days or even months to complete.

From the few papers[2,5–9] where experimental details of the ordering kinetics are given, it follows that in general the ordering is a two-stage process. In Ref. 6, the kinetics is described as a fast initial stage in which first-order liquid small-angle x-ray scattering peaks grow and then decrease, and a second stage in which Bragg scattering from the aggregates slowly builds up. In Ref. 9, local internal breathing relaxation processes and diffuse pattern relaxation modes have been identified experimentally. In many industrial applications—with fast processing demands—one can expect that incompletely relaxed structures are typical for quenched copolymer melts. In these applications, the structures are not in a state of lowest free energy, but rather in some frozen-in off-equilibrium state. In this paper, we will show that these imperfect transient states can be quantitatively modeled, using a density functional theory for the mesoscopic dynamic stability. The simulations demonstrate that the transient states evolve extremely slowly through a defect "annihilation" mechanism. This locks the system finally in metastable states with a few relatively well-ordered domains, which are separated by isolated defects.

Mean-field methods have been applied successfully to the description of equilibrium properties of the ordered phases, in particular, the phase diagrams and the density patterns of various types of copolymer melts (Refs. 10–12 and further references in Ref. 1). Especially, the early original studies of Helfand[10] (mostly strong segregation) and Leibler[11] (weak segregation) have contributed to our understanding of segregation phenomena. Much of the later theoretical work was based on these studies.[1] Also, in the present paper, we employ methods which can be traced back to the Helfand and Leibler studies, viz., the general form of the self-consistent field equations and the corresponding structure factors.

The mean-field methods have not yet been extended to models of the dynamic intermediate states, except for the analysis of Hashimoto;[8] this is essentially a linear Cahn–Hilliard[13] stability analysis of initial kinetics with the insertion of Leibler's structure factor for block copolymer melts.[11] The Hashimoto analysis is at least in qualitative agreement with the experiments reported in Ref. 7.

a)The author dedicates this work to the memory of Jan Scheutjens.

 0021-9606/93/99(11)/9202/11/$6.00 © 1993 American Institute of Physics

Fredrickson and Helfand[14] investigated the role of density fluctuations. The mean-field Leibler theory predicts that in case of symmetric block copolymer melts, the phase transition from the homogeneous to the lamellar state is second order.[11] The inclusion of fluctuations in the free energy functional makes the transition weak first order and suppresses the transition temperature. Because of the fluctuation-induced character of the transition, the nucleation barrier in an undercooled melt is relatively small.[15]

B. Principle of method

Density functional theory provides a general method for calculating the free energy in an inhomogeneous complex fluid. A recent overview[16] covers a larger number of different applications (extensive formal descriptions of the method can be found in Refs. 17–19). The present application to off-equilibrium systems of chain molecules is essentially a generalization of the classical Cahn–Hilliard approach,[13] along the lines pointed out some years ago by de Gennes.[20–22] The method applies to systems in which the collective diffusion phenomena are slow enough to ensure, at any given instant of time (on a time course-grained mesoscopic scale), a *unique* functional linkage between density profile and chain conformation distribution. The unique relation is not obvious. In systems in which relaxation phenomena are faster than the single chain relaxation time, the conformation distribution is not completely determined by the instantaneous interactions alone, but the linkage will depend on the kinetic pathway by which the system evolves. This fast kinetic limit is interesting in itself and will be studied in more detail in a following publication. Here, we confine ourselves to slow collective diffusion.

The essence of the dynamic density functional method is that the instantaneous unique conformation distribution can be obtained from the off-equilibrium density profile by coupling a fictitious external potential to the Hamiltonian, similar to the methods used in equilibrium models. It is important to realize that the (nonlinear) mapping between external potential and density profile is one to one.[18,19] There is only one unique external potential, and therefore conformation distribution, which minimizes the intrinsic free energy under the constraint that the distribution generates the density profile. Once the unique conformation distribution is known, the free energy can be calculated by standard statistical thermodynamics. The spatial gradient of the first functional derivative of the free energy with respect to the density (this derivative will be called *segmental* chemical potential) provides the driving force for diffusion. Following the Cahn–Hilliard reasoning, there will be a spontaneous flux from regions where the first functional derivative is high to regions where the derivative is low. Application to polymer systems results in generalized flux equations,[20–24] with phenomenological Onsager coefficients for the coupling between the thermodynamic forces and the ensuing fluxes. The inversion procedure by which the conformation distribution can be found from the density profile is of some importance. Tang and Freed[25] succeeded in a rigorous derivation of the de Gennes' prefactor of the Cahn–Hilliard square gradient term for homopolymer blends.[20,21] The so-called Flory–Huggins–de Gennes free energy functional has already been used in numerical studies of polymer phase separation kinetics.[26,27]

C. Computational aspects

Leibler[11] has shown that the free energy functional can be approximated (random phase approximation) by integration over a finite number of correlators; extensions of these correlators to general mixtures are available.[28] The original Leibler analysis is seminal for obtaining approximate analytical relations for the phase diagrams; the disadvantage is that it is limited to weak segregation phenomena only. Melenkevitz and Muthukumar[12] have extended the Leibler analysis to strong segregation phenomena by further numerical evaluation of the correlator integrals up to fourth order. As an alternative, we will demonstrate in this paper that for relatively short freely jointed chains, numerical inversion of the density functional is possible using finite element methods for any value of the interaction strength and without the truncation approximation inherent in the correlator methods. The numerical analysis has the additional advantage that extensions to more complex systems, e.g., multicomponent branched copolymer melts, are straightforward.

The crucial computer time consuming step in the present method is the inversion of the density functional. Every time step in the diffusion algorithm, a large system of equations has to be solved for the unique external field which determines the density profile. Fortunately, and this we want to emphasize, for small enough time steps, the inversion problem is reduced to zeroing repeatedly a well-behaved *linear* and *nonsingular* set of equations.

In contrast, the related *equilibrium* problem of finding the solution of the highly nonlinear self-consistent field equations is much more complicated. Lovett[29] emphasizes that many calculations of equilibrium density profiles have been made by iterating a nonlinear operator equation according to $\rho^{(n)}=\hat{\mathcal{T}}\rho^{(n-1)}$, where $\hat{\mathcal{T}}$ is the operator, ρ is the density profile (a function of spatial position), and superscript $^{(n)}$ is the nth estimate. These iterative procedures often oscillate wildly and fail to converge to a fixed point. Indeed, in the original classical analysis of Helfand,[10] considerable effort is devoted to the numerical procedures for calculation of the self-consistent-field density profiles in segregated block copolymer melts. On several occasions remarks are made that the numerical procedures are "out of the ordinary" [citation from Ref. 10(b)], involving expensive Newton iteration techniques. Newton methods are completely inadequate for the much bigger scale problems [zeroing $O(10^4$–$10^5)$ coupled equations $O(10^4$–$10^5)$ times] we are interested in.

In the present case of block copolymer melts, it can readily be shown that the same equations which lead to a unique solution in the nonequilibrium system lead to a multitude of self-consistent-field solutions in the equilibrium systems. These multiple equilibrium solutions are all true metastable states, separated by some (free) energy barrier. Thus our new dynamic density functional method

can be viewed from two perspectives. One is the physically intuitive point of view of relaxation through diffusion; the other is the mathematical perspective of the old *Jacobi method*[30] for solving (non)linear self-consistent-field equations by a relaxation algorithm. According to the later perspective, the dynamic density functional method provides a relaxation operator which transforms the density profiles from a state at time t to the state at time $t+\Delta t$. The dynamic (or relaxation) algorithm converges always, but, as in a real diffusion process, it converges more slowly the closer the system is to equilibrium.

Returning to the physical point of view, in complex systems, diffusion does not necessarily lead to the state of lowest free energy. Instead, the system may get locked in an intermediate metastable state; this is what we will find in the numerical simulations. Indeed, this is an obvious result. A copolymer melt can be considered a *complex* system, with many possible arrangements of off-equilibrium incompletely ordered microphases and many possible relaxation routes from disorder to order. It can intuitively be understood that the probability that a quenched melt relaxes to an perfectly ordered microphase of lowest free energy in a limited amount of time is practically zero. This is in line with a popular remark made by Prigogine that a sufficiently complex system is generally in a metastable state.[31]

D. Model description

The chain model is that of the freely jointed chain with a fixed bond length constraint. Backfolding is allowed. A drastic (but common) simplification is that in our model, the chains are not correlated through some chain–chain interaction term in the Hamiltonian. The mean field of the nonideal interactions is calculated by integration from the density profile.

On a mesoscopic coarse-grained time scale, the internal chain vibration modes are probably completely relaxed constantly. This means that for slow collective relaxation processes, a model like the constant bond length freely jointed chain which is used here is a more realistic choice than the Gaussian chain. Of course, the constant bond length freely jointed chain model cannot handle bond-elastic effects, e.g., bond stretching, but such effects will only be important in the presence of extremely strong shearing fields.

A further nontrivial advantage of the freely jointed chain over the Gaussian chain is that the Wageningen school[32] has provided efficient numerical algorithms for single chain statistics in external fields.[33] These algorithms apply to a variety of freely jointed chain models in lattice systems. The numerical algorithm of Scheutjens and Fleer for the generation of the conformation distribution of linear polymer chains in external fields has been used in the present study with only minor adaptions. The principle of the method (Green's functions propagation method) has a long history (cf. the remarks made in Ref. 34 and the textbooks[35,36]). The Scheutjens–Fleer algorithm is itself an adaptation of the early *matrix* theory of DiMarzio and Rubin.[37] Very similar "modified diffusion equations" linking the Green's functions have already been used by Helfand in the early 1970's.[10]

E. Outline of the paper

The dynamic variant of the density functional method for freely jointed chains in a mean-field environment is new. The extensive treatments of equilibrium applications of density functional theory in Refs. 16, 17, 19, 25, and 38 inspired the section "Dynamic Density Functional Theory." Earlier applications of density functional theory to Gaussian chains are, e.g., in Ref. 25, and for copolymer melts, the closely related random phase approximation analysis of Leibler.[11] The discussion of the Onsager coefficients is largely based on a paper by Kawasaki and Sekimoto.[23] In the "Results and Discussion" section, preliminary results are presented from integration of the collective diffusion equation on a pseudo-3D cubic lattice, where the gradients in one direction are neglected. For the kinetic coefficient, recourse is made to a local coupling model—this will be called the local coupling approximation. Reptation of the short chains is neglected. Fluctuations are introduced through an external Gaussian distributed random force, which is added to the deterministic thermodynamic force similar to the Cook method.[39]

F. Notation

The melt has volume V and contains n linear freely jointed chains. The chains are of diblock type $A_{N_A}B_{N_B}$ so that each chain has a block of N_A segments of type A connected to N_B segments of type B. The total length of the chain is $N=N_A+N_B$. The segment index number is $s=1,...,N$. The type of A or B segment is indexed by I or J, so that I or J points to either A or B. There are two external potential fields U_A for the A type segments and U_B for the B segments; similarly, the mean-field energetic interaction potentials are E_A and E_B and the ensemble averaged volume densities are ρ_A and ρ_B. The square brackets [ ] denote to a functional; the shorthand notation X denotes to the composite field $X_A(\mathbf{r})$, $X_B(\mathbf{r})$ (X is, e.g., ρ, U, or E), e.g., the free energy $F[X]$ denotes to the free energy functional $F[X_A,X_B]$ of the composite field X. The combination $\rho[U](\mathbf{r})$ indicates that ρ is a functional of U and as such a function of $\mathbf{r}$. $\beta=(k_BT)^{-1}$, $\mathbf{r}$ is a position in space, and t is time.

II. DYNAMIC DENSITY FUNCTIONAL THEORY

A. Partition function

The general partition functional Q for n chains in an external potential field U reads

$$Q[U]=\mathrm{Tr}\exp-\beta\left[H+\sum_{l=1}^{n}\sum_{s=1}^{N}U_s(\mathbf{R}_{s_l})\right], \tag{2.1}$$

where H is the Hamiltonian; U_s is U_A or U_B, depending on the type of segment s from chain l; and the trace Tr is the integration over phase space $\int(\cdots)d\mathbf{p}^{nN}\,d\mathbf{r}^{nN}$. In the remainder, we consider only interactions independent of the

momenta and limit the trace to integration over the coordinates. The interaction Hamiltonian is split in ideal and nonideal parts

$$H=H^{\mathrm{nid}}+H^{\mathrm{id}}. \tag{2.2}$$

In H^{id}, we count the connectivity interactions and collect in H^{nid} all the other interactions, e.g., excluded volume and energetic interactions. The partition functional is rewritten formally as

$$Q=Q^{\mathrm{id}}[U]\langle\exp-\beta H^{\mathrm{nid}}\rangle_U, \tag{2.3}$$

where the ideal partition functional Q^{id} is defined as

$$Q^{\mathrm{id}}[U]\equiv\mathrm{Tr}\exp-\beta(H^{\mathrm{id}}+U) \tag{2.4}$$

and the average $\langle\cdots\rangle_U$ is the ensemble average using the distribution function of the ideal chains in the external field. We introduce the mean-field interaction for the nonideal interactions

$$Q^{\mathrm{nid}}\equiv\langle\exp-\beta H^{\mathrm{nid}}\rangle_U\approx\exp-\beta V^{\mathrm{nid}}[\rho]\quad\text{(mean field)}, \tag{2.5}$$

where $V^{\mathrm{nid}}[\rho]$ is the average energy functional obtained from the nonideal interactions. The density ρ which is used as input for $V^{\mathrm{nid}}[\rho]$ is the ensemble averaged density, again using the distribution function of the ideal chains.

Thus, as a "gedanken experiment," the system is *virtually* divided in two subsystems. One is an ideal subsystem of n ideal chains in an external field with partition functional $Q^{\mathrm{id}}[U]$. The second subsystem contains all the nonideal interactions and has a partition functional $Q^{\mathrm{nid}}[\rho]$. Both subsystems evolve together as a function of time. At each instant of time, both partition functionals can be calculated from the momentous density fields, the ideal partition functional from inversion of the density functional (discussed below), and the nonideal partition functional directly through integration.

The total canonical partition functional Q of the system is obviously not constant. Indeed, in the spontaneous diffusion process, it will increase continuously. The rate with which Q changes follows from the diffusion algorithm to be discussed below.

B. Ideal partition functional

By definition, the ideal interaction H^{id} contains the connectivity interaction only. This automatically implies that the ideal interaction neglects the correlations between the chains, so that Q^{id} can be further factorized into single-chain partition functions $\Phi[U]$,

$$Q^{\mathrm{id}}[U]=\Phi[U]^n/n!. \tag{2.6}$$

The partition function $\Phi[U]$ of one ideal copolymer chain, subject to a composite external potential field $U=\{U_A,U_B\}$, is (cf. Ref. 36)

$$\Phi[U]=\frac{1}{(4\pi a^2)^{N-1}}\int_{V^N}\exp-\beta\Big[H^{\mathrm{id}}(\mathbf{R}_1,\ldots,\mathbf{R}_N)+\sum_{s=1}^{N}U_s(\mathbf{R}_s)\Big]D\mathbf{R}, \tag{2.7}$$

$$D\mathbf{R}\equiv\prod_{s'=1}^{N}d\mathbf{R}_s,$$

where $\mathbf{R}_s$'s are the coordinates of the segments, and U_s is U_A or U_B depending on the type of the segment s. H^{id} is an Edwards' connectivity Hamiltonian for the constant bond length freely jointed chain model

$$\exp-\beta H^{\mathrm{id}}(\mathbf{R}_1,\ldots,\mathbf{R}_N)=\prod_{s=2}^{N}\delta(|\mathbf{R}_s-\mathbf{R}_{s-1}|-a), \tag{2.8}$$

where a is the bond length.

The density functionals $\rho[U](\mathbf{r})$ are

$$\rho_I[U](\mathbf{r})\equiv C^0\cdot\sum_{s'=1}^{N}\delta^K_{Is'}\int_{V^N}\exp+\beta\Big(H^{\mathrm{id}}-\sum_{s=1}^{N}U_s\Big)\times\delta(\mathbf{r}-\mathbf{R}_{s'})\,D\mathbf{R}, \tag{2.9}$$

where δ^K is a Kronecker delta with value 1 if segment s' is of type $I(=A,B)$ and 0 otherwise, and C^0 is a normalization constant. In Appendix A is a standard numerical finite difference scheme (Green's propagation functions) for efficient calculation of the density functionals.

The intrinsic free energy of the ideal subsystem is

$$F^{\mathrm{id}}[\rho]=-\beta^{-1}n\ln\Phi+\beta^{-1}\ln n!-\sum_I\int_V U_I(\mathbf{r})\rho_I(\mathbf{r})d\mathbf{r} \tag{2.10}$$

with variation

$$\delta F^{\mathrm{id}}=-\sum_I\int_V U_I(\mathbf{r})\delta\rho_I(\mathbf{r})d\mathbf{r}. \tag{2.11}$$

C. Nonideal partition functional

The nonideal partition functional Q^{nid} of the mean-field pair interactions (2.5) is approximated as

$$Q^{\mathrm{nid}}=Q_0\exp-\Big[\frac{\beta}{2}\sum_I\int_V E_I(\mathbf{r})\rho_I(\mathbf{r})d\mathbf{r}\Big], \tag{2.12}$$

where Q_0 is a nonessential constant and the interaction fields E are defined as

$$E_I(\mathbf{r})\equiv\frac{\beta^{-1}}{4\pi a^2}\sum_J\chi_{IJ}\int_V\delta(|\mathbf{r}-\mathbf{r}'|-a)\rho_J(\mathbf{r}')d\mathbf{r}' \tag{2.13}$$

(see Appendix A for the numerical calculation method). χ_{IJ}'s are generalized Flory–Huggins parameters[42]

$$\chi_{IJ}=\begin{cases}\chi, & \text{if } I\neq J\\ 0, & \text{if } I=J\end{cases} \tag{2.14}$$

The free energy of the nonideal subsystem is:

$$F^{\mathrm{nid}}\equiv-\beta^{-1}\ln Q^{\mathrm{nid}} \tag{2.15}$$

$$=-\beta^{-1}\ln Q_0+\frac{1}{2}\sum_I\int_V E_I(\mathbf{r})\rho_I(\mathbf{r})d\mathbf{r} \tag{2.16}$$

with the variation

$$\delta F^{\mathrm{nid}}=\sum_I\int_V E_I(\mathbf{r})\delta\rho_I(r)dr. \tag{2.17}$$

D. Free energy functional

The total free energy functional $F[\rho]$ is the sum of the free energies of the ideal and nonideal subsystems (2.10) and (2.16)

$$F[\rho] \equiv -\beta^{-1} \ln Q^{\mathrm{id}} - \beta^{-1} \ln Q^{\mathrm{nid}} \tag{2.18}$$

$$= F^{\mathrm{nid}}[\rho] + F^{\mathrm{id}}[\rho]. \tag{2.19}$$

Similarly, the variation of the free energy is obtained by addition of the subsystem variations (2.11) and (2.17)

$$\delta F = \sum_I \int_V \mu_I(\mathbf{r}) \delta\rho_I(\mathbf{r}) d\mathbf{r}, \tag{2.20}$$

where we have introduced the *segmental* chemical potential μ_I,

$$\mu_I \equiv E_I(\mathbf{r}) - U_I(\mathbf{r}). \tag{2.21}$$

Notice the difference between the definitions of the *segmental* and the usual *polymer* chemical potentials. The segmental chemical potential refers to the shift in free energy when the ensemble averaged density of the segments decreases or increases *locally*. The classical polymer chemical potential refers to the case that chain molecules are added or removed from the *entire* system. Basically, what we have done here is separate the free energy functional in a purely ideal mixing entropy part F^{id} for chain molecules and a nonideal part F^{nid} for the mixing energy. In this picture, the inverse $U[\rho]$ functional can be interpreted as a kind of partial segmental entropy of mixed chain molecules.

If we take a wider point of view, result (2.20) is *not* at all surprising. It is a simple presentation of the very general "fundamental equation in the theory of nonuniform liquids" (citation from Evans' paper[17]) derived through classical density functional theory. The fundamental equation states that the first variation of the (Helmholtz) free energy (the so-called *intrinsic* chemical potential μ_{in}) is identical to $-U$, where it is understood that in the corresponding Hamiltonian, all correlations are taken into account. The intuitive notion is that the effective external potential is shifted from the fully correlated value U to $U-E$ in a mean-field environment.

E. Diffusion equation

There has been ample discussion regarding the appropriate form of the diffusion equation for polymer morphology dynamics.[20–24] From the discussions, it is clear that there are three effects which are important:

(I) In an incompressible system, there is obviously always a backflow such that the net total flux is zero. The backflow can easily be incorporated in the diffusion equation by an extra external pressure field which constrains the fluxes.[20–22] In our case, where we have two components A and B, the result is a reduced flux equation with only one net thermodynamic force, namely, the gradient of an exchange chemical potential μ. Here, we define μ with respect to the potentials of the B segments

$$\mu \equiv \mu_A - \mu_B. \tag{2.22}$$

(II) The Onsager kinetic coefficients are in principle not simple scalar quantities, but operators which depend in some way on the conformation distribution, and therefore indirectly in a functional sense on the density pattern. Kawasaki and Sekimoto[23] obtained an explicit expression for the kinetic operators for the reptation model in terms of derivatives of single chain density–density correlation functions. From their analysis, it follows immediately that in this case, the fluxes in the disordered state are kinetically coupled on the length scale of the random coil size. This result was essentially also obtained by the earlier studies which applied to the disordered state only.[20–24] The approach of Kawasaki and Sekimoto allows in principle the calculation of the Onsager kinetic coefficient as a functional of the density because the density–density correlations can be described as functionals of the densities. However, this leads to considerable numerical difficulties, so that we will not pursue this approach further.

For the short freely jointed chains, we introduce an extreme *ad hoc* simplification—the *complete* neglect of kinetic coupling between the segments. Although this local coupling approximation (LCA) may seem unrealistic, remember that the thermodynamic coupling through the density functional remains, so that even with kinetic decoupling, it will be impossible that A type segments diffuse independent from the B type segments.

The equations for the LCA are

$$\Lambda_{IJ}(\mathbf{r},\mathbf{r}') = \begin{cases} 0, & \text{if } I \neq J, \\ D\delta(\mathbf{r}-\mathbf{r}')\rho_I(\mathbf{r}'), & \text{if } I = J, \end{cases} \tag{2.23}$$

$$\Lambda(\mathbf{r},\mathbf{r}') = D\delta(\mathbf{r}-\mathbf{r}')\rho_A(\mathbf{r}')\rho_B(\mathbf{r}') \tag{2.24}$$

where D is a segmental diffusion constant and Λ_{IJ} is the Onsager kinetic coefficient.

(III) Cook[39] introduced a stochastic Langevin force in the original Cahn–Hilliard analysis. The thermal fluctuation term has been found to be essential for preventing freezing-in effects in domain formation in previous studies of demixing of polymer blends.[27] Following this approach, we have the stochastic diffusion equation

$$\frac{\partial \rho_A}{\partial t} = D\nabla\rho_A(1-\rho_A) \cdot (\nabla\mu + \nabla\tilde{\eta}), \tag{2.25}$$

where we have used the LCA for the kinetic coefficient and $\nabla\tilde{\eta}$ is the random force. From the fluctuation–dissipation theorem,[43–46] it follows that the distribution of $\tilde{\eta}$ must be Gaussian distributed white noise with moments

$$\langle \tilde{\eta}(\mathbf{r},t) \rangle = 0, \tag{2.26}$$

$$\langle \tilde{\eta}(\mathbf{r},t)\tilde{\eta}(\mathbf{r}',t') \rangle = 2\beta^{-1}\delta(\mathbf{r}-\mathbf{r}')\delta(t-t'). \tag{2.27}$$

III. RESULTS AND DISCUSSION

We discuss here a few numerical results qualitatively for the purpose of demonstration of the method in Ref. 47. A full comparative analysis with experimental results reported in Ref. 9 (dynamic structure factors) of these and other results will be in a following paper.

In Figs. (1a) and (1b) is depicted the time evolution of density patterns in copolymer melts, obtained by numerical integration of the diffusion equation through a finite difference scheme (the explicit forward time centered space algorithm[30]). The system is a quenched symmetric A_8B_8 [Fig. 1(a)] and asymmetric A_6B_{10} [Fig. 1(b)] copolymer melt. The simulations are based on a 3D cubic lattice, where we have neglected the gradients in one dimension—this provides formulas for a pseudo-3D calculation on a 2D grid (Appendix A). The periodic lattice contains 64^2 rectangular cells of size a^2. The dimensionless time step $\Delta\tau = (D\Delta t)/a^2$ in the integration is 0.01. Every time step, the external fields are iterated until the density functional matches the current density profile within a relative deviation (root mean square) $\Delta \ln \rho = 0.01$ (Appendix B). The simulations required two to three CPU days calculation time on a workstation.

The quench is instantaneous on $\tau=0$ from $\chi=0$ to $\chi=1$. The start configuration is the homogeneous profile $\rho_A(\mathbf{r})=N_A/N$; $\rho_B(\mathbf{r})=N_B/N$. There is no preequilibration with respect to the fluctuations at $\chi=0$ before the quench. Separate runs showed that in the absence of interactions, the homogeneous system reaches fluctuation equilibrium within a few hundred diffusion steps; this is a few units of time on the scale in Fig. 1.

The spinodal for these short freely jointed chains is at a slightly different interaction parameter than would be expected from application of Leibler's formula for long Gaussian chains. For derivation of the inverse structure S_q^{-1} for our system, we refer to Appendix C. We find that for $\chi=1$, the inverse structure factor is negative for wavelengths λ in the intervals (in units of (a) $\lambda\in\{4.3,9.2\}$ (A_8B_8) and (b) $\lambda\in\{4.8,8.0\}$ (A_6B_{10}) and positive outside these intervals. At the spinodal, the critical wavelength is found from the root $S_{q_s}^{-1}=0$; the critical values are $\lambda_s=6.15$, $\chi_s=0.79$ (A_8B_8) and $\lambda_s=6.11$, $\chi_s=0.90$ (A_6B_{10}). The critical interaction value $\chi N=16$ is relatively small in both cases, so that we are still close to the weak segregation limit. Application of the Leibler formula (4.6) from Ref. 11 gives $\lambda_s^{\text{Leib}}=5.27$, $\chi_s^{\text{Leib}}=0.66$ (A_8B_8) and $\lambda_s^{\text{Leib}}=5.20$, $\chi_s^{\text{Leib}}=0.74$ (A_6B_{10}). The nonlocal interaction and the constant bond length constraint in our freely jointed chain model shifts the spinodal slightly upwards and to longer wavelengths compared to the Leibler result, but the difference is not very large. For long chain lengths, our structure factor reduces exactly to Leibler's equation (Appendix C).

A few conspicuous features emerge.

(I) Because of the neglect of the gradients in the third dimension, the "strings" in Fig. 1(a) may be interpreted as cross sections of infinitely large lamellas and the "dots" in Fig. 1(b) as cross sections of infinitely long cylinders. Qualitatively, these structures can readily be understood from the phase diagrams reviewed in Ref. 1. The A blocks and B blocks are connected by chemical bonds in single chains and this makes macroscopic phase separation impossible. Rather, the blocks form microdomains, separated on the scale of the average coil size. In the A_8B_8 melt, the phase separation necessarily leads to a locally symmetric segregation of A rich and B rich domains; these are the labyrinth structures in Fig. 1(a). In the A_6B_{10} segregating melt, the B domains must be larger than the A domains in view of the asymmetry of the block sizes. In case of strong interactions, the asymmetric system may try to minimize unfavorable contacts by the formation of asymmetric lamellas, but this costs relatively much entropy. Here the interactions are still relatively weak, so that a situation is favored in which B rich domains enclose A rich domains, and this leads to the irregular hexagonal dot patterns in Fig. 1(b).

(II) Initially, what we observe for time $\tau\leqslant 30$ is a deepening of correlation holes. In the spirit of the Cahn–Hilliard–Cook analysis, in this linear regime, unstable fluctuations with wavelengths in the critical unstable window where the inverse structure factor is negative grow roughly exponentially. This regime is identical to the regime analyzed before by Hashimoto[8] with time-dependent Ginzburg–Landau theory, using Leibler's structure factor.

(III) In both systems, the fast initial phase-separation kinetics comes to an almost complete and abrupt halt in a nonperfect defect-rich transient state, which evolves further through an extremely slow defect annihilation mechanism. This is the interesting nonlinear regime. In the frames, there are several examples where nearby "hot spots," i.e., sites of high free energy density such as sharp bends, disconnected edges, or disconnected cylinders suddenly merge, whereby the total free energy is lowered. The annihilation mechanism slows down considerably as the number of defects decreases. The last frames already have a few near-perfect domains, separated by dislocations or isolated defects. As we have discussed before in the Introduction, these type of "poorly defined morphologies" should be typical for shear-free quenched (block) copolymer melts.

(IV) There is a peculiar long-term memory effect. Even in the symmetric block copolymer melt, which we expect to evolve to a distinct lamellar state, the final frames have some *hexagonal* character, reflected by the presence of 120° bends in the lamellas. Close inspection of the frame at the end of the linear regime $\tau=30$ shows that initially the deepening correlation holes first quickly rearrange to an intermediate hexagonal type packing. This packing is apparently temporarily more favorable than a lamellar packing. The conjecture is that in a 3D system, a *cubic* packing could temporarily be more favorable. In the second transient phase, the hexagonal packing then dissolves and is slowly transformed into a lamellar packing. Obviously, in this case it takes an extremely long time before the transient hexagonality has completely disappeared by the defect annihilation mechanism.

General remarks: The present method suffers from a number of conceptual deficiencies; we list here the most important ones:

(I) Foremost, the separation between purely entropic and purely energetic effects is unrealistic in case of strong ordering phenomena. For example, the complete loss of chain–chain correlations in the interaction Hamiltonian has as a consequence that the chains have far too much

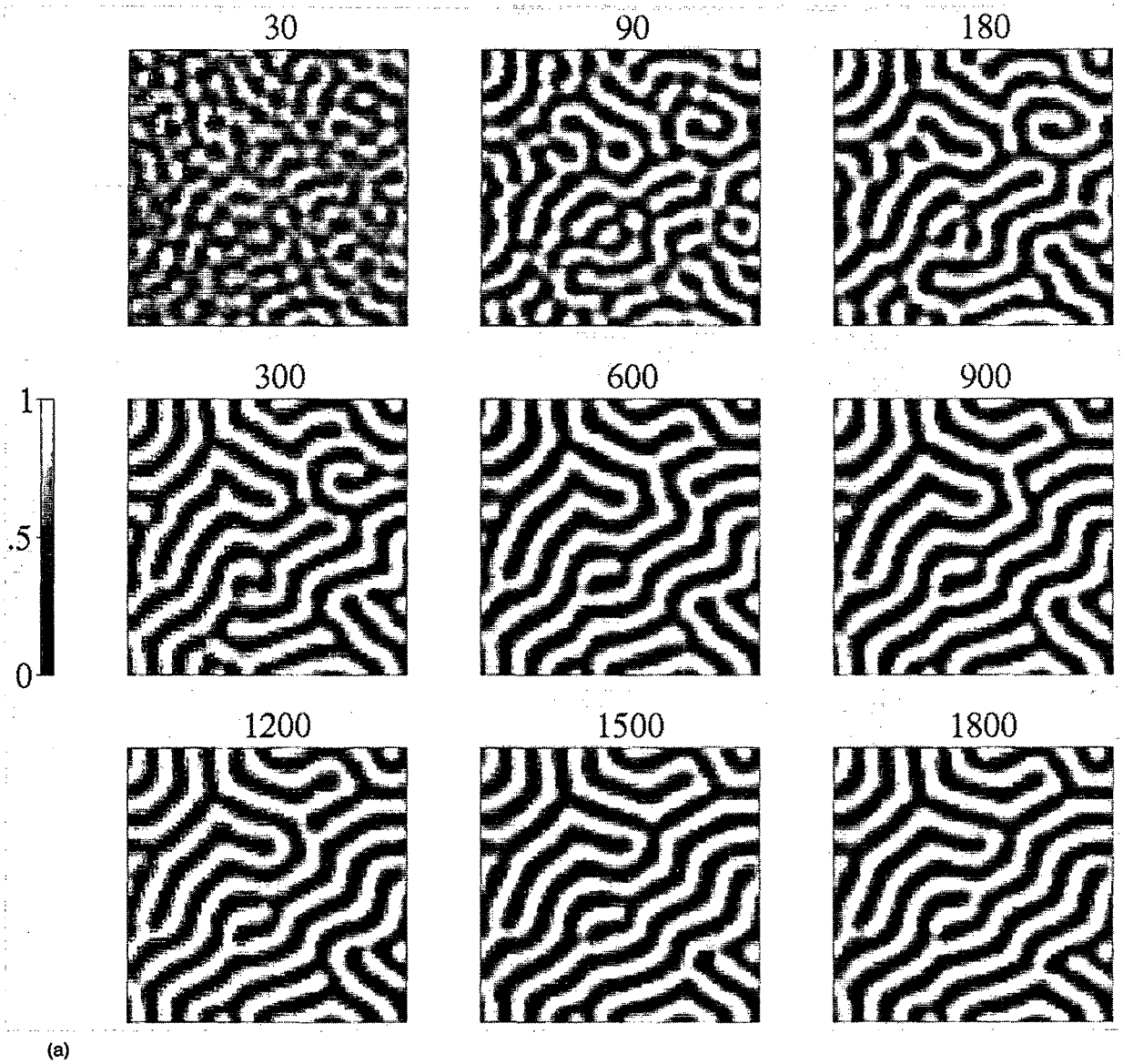

FIG. 1. Temporal and spatial evolution of density field $\rho_A(\mathbf{r}, t)$ in the disorder–order phase transition of (a) symmetric A_8B_8 and (b) asymmetric A_6B_{10} diblock copolymer melts. On $\tau=0$, the interactions are instantaneously increased from $\chi=0$ (ideal disordered system) to $\chi=1$, slightly above the spinodal. The dimensionless time $\tau=Dt/a^2$ is indicated above the frames. The density field on time $\tau+\Delta\tau$ is calculated from the density field on τ by a forward time centered space finite difference integration of the diffusion relaxation equation (pseudo-3D algorithm). The periodic lattice measures 64^2 sites of size a^2. The time increment $\Delta\tau=0.01$.

configurational freedom, which introduces an unphysical too large entropical resistance to big changes in the conformation distribution. This effect has been observed by Leermakers using the self-consistent-field Scheutjens–Fleer calculations for density profiles in lipid membranes.[32(c)] We know from de Gennes' work[35] that close to the disordered state, ideal chain statistics is a good approximation, but these arguments apply only to (very) long chains, whereas here we study short chains. Although it is in principle not impossible to include chain–chain correlation effects in the present analysis, e.g., by retaining excluded volume interactions between two chains explicitly in the ideal part of the Hamiltonian (this of course redefines the fields U and E), it is at the moment questionable whether these extensions can be cast in efficient numerical procedures.

(II) A related neglected effect is the *intra*chain correlation. We have here used a freely jointed chain model for short chains. If we interpret the results as to apply to longer chains, with a monomer identified as a Kuhn statistical unit, or even as a "blob" in the de Gennes model, then we face at once the difficulty that we have completely neglected the internal eleasticity of the statistical unit by using a constant bond length model. As is well known, a Gaussian chain model is a better choice for connected, elastic units. The entropic elasticity of the statistical unit has a consequence that a perturbation applied to a certain unit needs a certain time to propagate along the chain. This

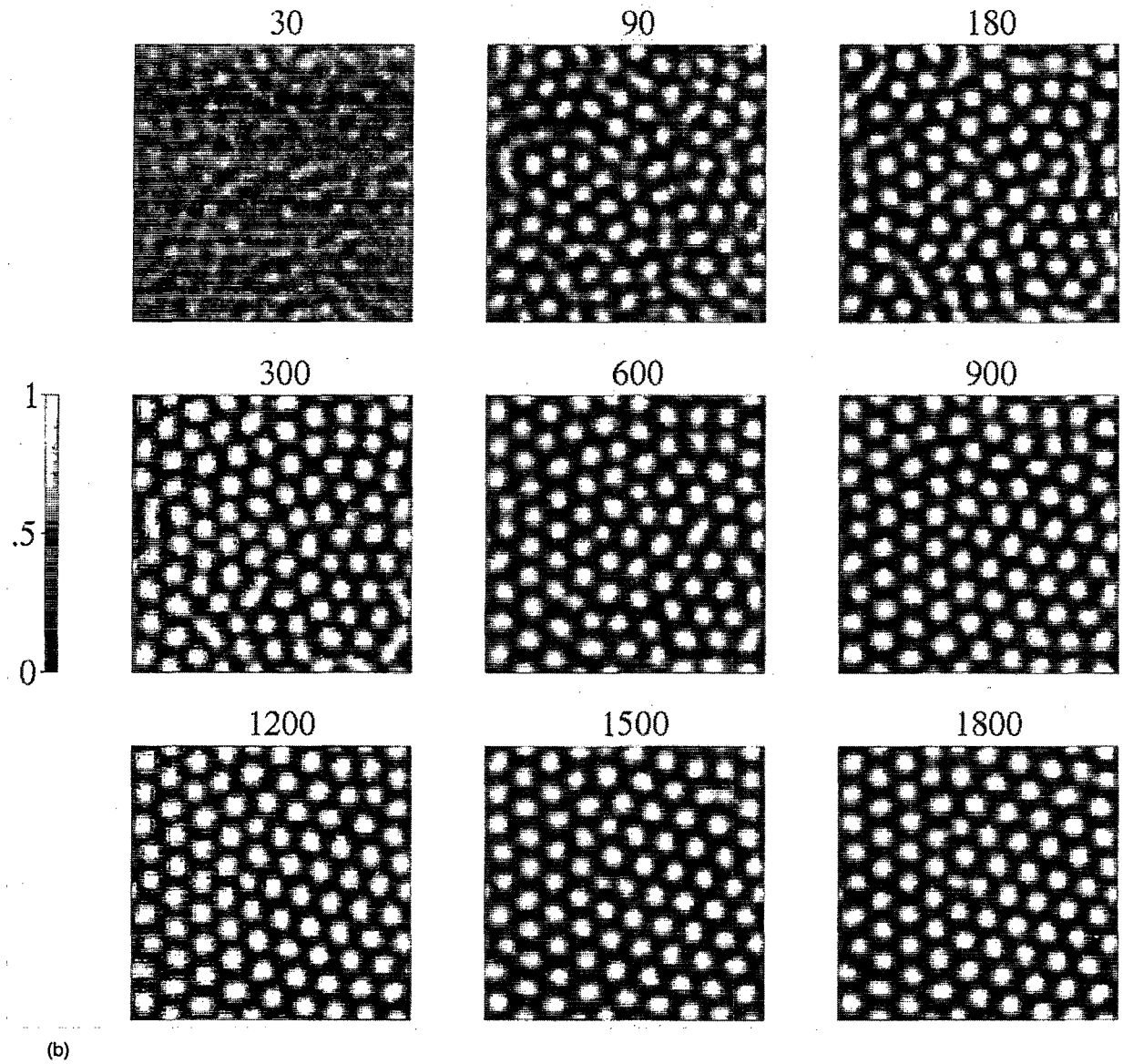

FIG. 1. (*Continued.*)

introduces a history dependence of fluxes (velocities of the units) and this in turn leads to an elastic, time-dependent kinetic coefficient.

Returning to the interaction Hamiltonian, if we use the freely jointed chain model for short chains, e.g., oligomeric surfactants, with a monomer interpreted as a small rigid unit, e.g., a–C_{H_2}–unit, then we encounter the problem that we have completely neglected bond angle constraints, so that again our chain model is too flexible. We could use a connectivity Hamiltonian with fixed bond angles to alleviate this problem.

(III) We are currently investigating more closely the kinetic coefficients for the freely jointed chain model. Stricktly speaking, on a molecular time scale, the rigid mechanical coupling between the beads in a constant bond length freely jointed chain model has as a consequence that the coupling between forces and velocities of the beads is instanteneous; there are in this model no elastic elements as in the Gaussian model. It is, however, clear that in the thermodynamic limit, we should consider the external potential and density fields as the collective variables rather than the individual actions of the beads. We have tested the dynamical coupling between the beads in a simple freely jointed chain model by a Stokes dynamics simulation [Bekker (work in progress)]. If we then consider an ensemble of these chains and calculate the average response of the velocities to a infinitisemal external force applied to one of the beads, we find that on the average, the decay length of the *instanteneous* kinetic coefficient is only a few segment lengths. Although this would seem to favor the simple local coupling approximation we have proposed in this paper, the local coupling cannot be correct on longer time scales. Binder[22] gave some convincing arguments that for short Gaussian chains in the Rouse dynamics limit, the long time kinetic coeffient has a decay length on the scale of the radius of gyration similar to reptating chains.

(IV) A fourth deficiency is that it is not yet clear what the smallest time scale of the simulations must be. We have argued that the collective dynamics must be slow enough to ensure applicability of the Boltzmann statistics at every instant of time on a mesoscopic coarse-grained time scale. A somewhat crude argument could be that we must have $\Delta\tau \gg \tau_c$, the single chain relaxation time. For short chains in the disordered melt, we could use $\tau_c \approx R_g^2/D_g \sim N^2$ as a typical relaxation time for the conformation distribution. However, in the ordered state, the relaxation time τ_c may be much larger. This problem, closely related to the exact functional form of the kinetic coefficient, is at the moment not yet resolved satisfactorily. Erukhimovitch and Semenov[24] study the dynamics of collective fluctuations with a history dependent kinetic coefficient (reptation model), but this applies to small perturbations in homogeneous blends only. Here, the repercussions are that an instantaneous quench as we have performed could in some cases yield unrealistic results, especially in the initial stage of the kinetics. For example, from the Cahn–Hilliard analysis, it follows that in the local coupling approximation the spatial frequency $q_{\max}$ of the fastest unstable density fluctuation is at the maximum of $q^2 S_q^{-1}$. For a very deep quench, this would imply that $q_{\max} \sim a^{-1}$; this is on the scale of the *monomer* size, rather than the scale of the coil size, and this leads to the conclusion that for these systems, we would need to include relaxation mechanisms on a monomer length and time scale.

It is very questionable whether the Boltzmann statistics is applicable to the rapid evolving transient states on monomer time and length scales. However, the numerical results indicate that soon after the quench, the mesoscopic dynamics turns into extremely slow relaxation processes of big collective structures, in agreement with many experimental findings. For these length and time scales, the present method is especially suited. In a sense, we need the thermodynamic potentials on a microscale to find the properties on the mesoscale. Intuitively, we expect that the relaxation mechanisms of the global structures on a mesoscale should be relatively independent of the precise description of the microscale, as long as we keep the most essential microinteractions; in the case of copolymer melts, this is the connectivity of dissimilar segment types, but, as we have neglect almost all micro degrees of freedom, we should not overinterpret the results on small length and time scales.

IV. CONCLUSION

The mesoscopic dynamics of slow collective diffusion phenomena in block copolymer melts can be modeled numerically with a mean-field dynamic density functional approach. The numerical inversion of the density functionals is stable. Preliminary numerical results indicate that the present method is capable of generating defect-rich transient states, which may eventually lock into metastable states, similar to incompletely relaxed systems found in many industrial applications. The algorithms can be readily extended to more complex systems, e.g., multicomponent branched copolymer mixtures. The separation of purely entropic and purely energetic interactions limits for the moment quantitative predictions to relatively weakly ordered systems.

ACKNOWLEDGMENTS

I appreciate many encouraging discussions with the late Jan Scheutjens in the initial phase of this work. Frans Leermakers (Wageningen Agricultural University) and Olaf Evers (BASF) are acknowledged for critically reading the manuscript and useful comments. Rein van der Hout, Piet den Dekker, and Chiel van Hemert (Akzo) were instrumental in software development and application of the theory to a variety of complex industrial systems. Akzo research management is acknowledged for support while the author was in the Department of Applied Mathematics of Akzo Research Laboratories in Arnhem, The Netherlands, where this study was initiated.

APPENDIX A: CALCULATION OF THE DENSITY FUNCTIONALS

1. Calculation of the densities from the external fields

On a 3D cubic grid of lattice sites of size a^3, the algorithm for the calculation of the density functionals is as follows: We scale the Cartesian coordinates x, y, and z of all the 3D fields with the segment size

$$x \to x/a, \tag{A1}$$

$$y \to y/a, \tag{A2}$$

$$z \to z/a, \tag{A3}$$

and approximate the connectivity delta operator by a finite difference scheme for a cubic lattice

$$\frac{1}{4\pi a^2}\int_V \delta(|\mathbf{r}-\mathbf{r}'|-a)\cdot X(\mathbf{r}')\cdot dr'$$

$$\to \frac{1}{6}[X(x-1,y,z)+X(x+1,y,z)+X(x,y-1,z)$$

$$+X(x,y+1,z)+X(x,y,z-1)+X(x,y,z+1)] \tag{A4}$$

(X is here an arbitrary field). In the pseudo-3D algorithm, we neglect any gradients in the third direction z, in this case,

$$X(x,y,z-1)=X(x,y,z+1)=X(x,y,z), \tag{A5}$$

which results in effective 2D recurrence relations for the (once integrated) Green's propagation functions[32,35,36]

$$G(x,y,s)=\tfrac{1}{6}\exp-\beta U_s(x,y)\cdot[G(x-1,y,s-1)+G(x+1,y,s-1)+G(x,y-1,s-1)+G(x,y+1,s-1)+2G(x,y,s-1)], \quad \text{(A6)}$$

$$G^{\text{inv}}(x,y,s)=\tfrac{1}{6}\exp-\beta U_s(x,y)\cdot[G^{\text{inv}}(x-1,y,s+1)+G^{\text{inv}}(x+1,y,s+1)G^{\text{inv}}(x,y-1,s+1)+G^{\text{inv}}(x,y+1,s+1)+2G^{\text{inv}}(x,y,s+1)]. \quad \text{(A7)}$$

Notice that in a true 2D algorithm, we would have omitted the central terms $G(x,y,s-1)$ and $G^{\text{inv}}(x,y,s+1)$. On the periodic lattice of $M = L*L$ grid points, we let the indices of x and y run from 0 to $L+1$ and set for all the fields the boundary values according to the periodic boundary conditions, e.g., $X(0,y)=X(L,y)$.

The partition function is calculated from

$$\Phi=\sum_{x=1}^{x=L}\sum_{y=1}^{y=L}G(x,y,N)=\sum_{x=1}^{x=L}\sum_{y=1}^{y=L}G^{\text{inv}}(x,y,1) \quad \text{(A8)}$$

and the densities of the I-type segments from

$$\rho_I(x,y)=\frac{n\nu}{\Phi}\sum_{s=1}^{N}\delta_{Is}^{K}\cdot\exp+\beta U_s(x,y)\cdot G(x,y,s)\cdot G^{\text{inv}}(x,y,s), \quad \text{(A9)}$$

where δ_{Is}^{K} is the Kronecker delta with value 1 if segment s is of type I and 0 otherwise. In the incompressible system, we can easily calculate the number of chains by $n\nu=V/N$. On the scaled lattice, the segment volume ν is unity and hence $n=M/N$.

2. Calculation of the nonideal interaction fields from the densities

The mean field interaction fields are calculated by

$$\beta E_I(x,y)=\frac{1}{6}\sum_J\chi_{IJ}[\rho_J(x-1,y)+\rho_J(x+1,y)+\rho_J(x,y-1)+\rho_J(x,y+1)+2\rho_J(x,y)] \quad \text{(A10)}$$

APPENDIX B: INVERSION OF DENSITY FUNCTIONAL

We define a composite auxilliary field W,

$$W(\mathbf{r})=[W_A(\mathbf{r}),W_B(\mathbf{r})]. \quad \text{(B1)}$$

The field is constructed such that it depends *parametrically* on an arbitrary density profile $\rho' = \rho'_A(\mathbf{r})$, $\rho'_B(\mathbf{r})$ and *functionally* on the external potentials through the density functionals $\rho=\rho_A(\mathbf{r})$, $\rho_B(\mathbf{r})$ of Eq. (II.9):

$$W_I(\mathbf{r})\equiv-\ln\frac{\rho_I(U)(\mathbf{r})}{\rho'_I(\mathbf{r})}+\frac{\beta}{V}\int_V U_I(\mathbf{r})d\mathbf{r}. \quad \text{(B2)}$$

The density profiles $\rho'_I(\mathbf{r})$ are (weakly) restricted by one condition, namely, that the total number of segments contained in $\rho'_I(\mathbf{r})$ must be equal to the number of I segments present in the system

$$\int_V\rho'_I(\mathbf{r})d\mathbf{r}=\frac{N_I}{N}V. \quad \text{(B3)}$$

In the root $W\equiv0$, the external potential generates $\rho[U]=\rho'$ under the constraint that the average field is zero (this constraint prevents drifting of the external potential reference levels).[40] From application of the classical one-to-one mapping theorem from density functional theory (Ref. 18 and a particular elegant proof in Ref. 19), we know that the inverse of the density functional is *unique*. The divergence operator in the diffusion algorithm (forward time centered space) ensures that the densities ρ' are updated each time step in such a way that condition (B3) is obeyed continuously. Notice further that the derivative matrix of W is positive definite *always*[41]

$$\frac{\delta W_I(\mathbf{r})}{\delta U_J(\mathbf{r}')}=\frac{\beta\nu\tilde{G}_{I,J}^{(2),\text{id}}(\mathbf{r},\mathbf{r}')}{\rho_I[U](\mathbf{r})}+\frac{\beta\delta_{IJ}^{K}}{V}, \quad \text{(B4)}$$

where $\tilde{G}_{I,J}^{(2),\text{id}}$ is the positive definite density–density correlation of the ideal chain and ν is the segment volume. In practice, we choose a small time step so that the problem of inversion is reduced to reversing repeatedly a linear, nonsingular set of equations.

In the reported simulations, we used an allowed root mean square deviation from the root $\Delta W\approx\Delta\ln\rho<\epsilon=0.01$. This seems rather rough, but smaller values of ϵ gave essentially identical results. The reason is that the attained error in the external field is $O(\epsilon/N)$ (in weakly ordered systems), so that any increased accuracy in the external fields obtained by using a tighter criterion is negligible compared with the noise introduced by the random term.

APPENDIX C: STRUCTURE FACTOR HOMOGENEOUS STATE

We employ here the standard RPA calculation method.[35] There are two small differences with the Leibler approach:[11] (i) here we use a nonlocal, nonideal interaction and (ii) we have a freely jointed chain model rather than a Gaussian chain model. A combination of ideal and nonideal responses in the standard way for incompressible systems[11,35] results in the well-known mean-field expression for the structure factor

$$S_q^{-1}\equiv-2w_q\chi+S_q^{0-1}, \quad \text{(C1)}$$

where q is here the length of the wave vector $\mathbf{q}$. The ideal structure factor is

$$S_q^0\equiv\frac{S_{AA}^0S_{BB}^0-S_{AB}^0S_{BA}^0}{S_{AA}^0+S_{AB}^0+S_{BA}^0+S_{BB}^0} \quad \text{(C2)}$$

and the unconstrained response functions of the ideal freely jointed chain in the homogeneous state S_{IJ}^0 are

$$S^0_{IJ}(q) \equiv -\beta^{-1} \frac{\delta \rho_I(q)}{\delta U_J(q)} \tag{C3}$$

$$= \frac{1}{N} \sum_{s=1}^{N} \sum_{s'=1}^{N} \delta^K_{Is} \delta^K_{Js'} w_q^{|s-s'|}. \tag{C4}$$

The coupling term w_q is defined as the Fourier transform of the delta connectivity operator.[36]

$$w_q \equiv \sin qa/q. \tag{C5}$$

The connection with the Leibler formulas, e.g., Eq. (IV-6) from Ref. 11, is evident if we consider the limit of long chain lengths N, N_A, $N_B \gg 1$, and wave vectors smaller than the reciprocal monomer size $qa \ll 1$. The limiting behavior is

$$2\chi w_q \to 2\chi \tag{C6}$$

and (cf. Ref. 36)

$$w_q^{|s-s'|} \to \exp -y|s-s'|, \tag{C7}$$

where $y = q^2a^2/6$. These limits correspond exactly with, respectively, the behaviors of local nonideal interactions and ideal correlations in the Gaussian chain model which have been used by Leibler.[11]

[1] F. S. Bates and G. H. Fredrickson, Annu. Rev. Phys. Chem **41**, 525 (1990).
[2] F. S. Bates, J. H. Rosedale, and G. H. Fredrickson, J. Chem. Phys. **92**, 6255 (1990); J. H. Rosedale and F. S. Bates, Macromolecules **23**, 2329 (1990).
[3] T. Hashimoto, M. Shibayama, and H. Kawai Macromolecules **13**, 1237 (1980); T. Hashimoto, M. Shibayama, M. Fujimara, and H. Kawai, in *Block Copolymers—Science and Technology*, edited by D. J. Meier (Harwood, London, 1983) p. 63.
[4] G. Hadziioannou, C. Picot, A. Skoulios, M.-L. Ionescu, A. Mathis, R. Duplessix, Y. Gallot, and J.-P. Lingelser, Macromolecules **15**, 263 (1982); G. Hadziioannou and A. Skoulios, *ibid.* **15**, 267 (1982); **15**, 271 (1982).
[5] M. Schuler and B. Stuhn, Macromolecules **26**, 112 (1993).
[6] C. R. Harkless, M. A. Singh, and S. E. Nagler, Phys. Rev. Lett **64**, 2285 (1990).
[7] J. G. Connel and R. W. Richards, Polymer **32**, 2033 (1991).
[8] T. Hashimoto, Macromolecules **20**, 456 (1987).
[9] S. H. Anastasiadis, G. Fytas, S. Vogt, and E. W. Fischer, Phys. Rev. Lett. **70**, 2415 (1993).
[10] E. Helfand, Macromolecules **80**, 552 (1975); E. Helfand and Z. R. Wasserman, Macromolecules **9**, 879 (1976).
[11] L. Leibler, Macromolecules **13**, 1602 (1980).
[12] J. Melenkevitz and M. Muthukumar, Macromolecules **24**, 4199 (1991).
[13] J. W. Cahn and J. Hilliard, J. Chem. Phys. **28**, 258 (1958); J. W. Cahn, *ibid.* **42**, 93 (1965).
[14] G. H. Fredrickson and E. Helfand, J. Chem. Phys. **87**, 697 (1987).
[15] G. H. Fredickson and K. Binder, J. Chem. Phys. **91**, 7265 (1989).
[16] *Fundamentals of Inhomogeneous Fluids*, edited by D. Henderson (Marcel Dekker, New York, 1992).
[17] R. Evans, Adv. Phys. **28**, 143 (1979).
[18] J. T. Chayes and L. Chayes, J. Stat. Phys. **36**, 471 (1984).
[19] N. D. Mermin, Phys. Rev. A **137**, 1441 (1965).
[20] P.-G. de Gennes, J. Chem. Phys. **72**, 4756 (1980).
[21] P. Pincus, J. Chem. Phys. **75**, 1996 (1981).
[22] K. Binder, J. Chem. Phys. **79**, 6387 (1983).
[23] K. Kawasaki and K. Sekimoto, Phys. Status Solidi A **148**, 361 (1988); **143**, 349 (1987).
[24] I. Y. Erukhimovich and A. N. Semenov, Sov. Phys. JETP **63**, 149 (1986).
[25] H. Tang and K. F. Freed, J. Chem. Phys. **94**, 1572 (1990).
[26] A. Chakrabarti, R. Toral, J. D. Gunton, and M. Muthukumar, Phys. Rev. Lett. **63**, 2072 (1989); M. A. Kotnis and M. Muthukumar, Macromolecules **25**, 1716 (1992).
[27] G. Brown and A. Chakrabarti, J. Chem. Phys **98**, 2451 (1993).
[28] A. V. Dobrynin and I. Ya Erukhimovitch, Macromolecules **26**, 276 (1993).
[29] R. Lovett, J. Chem. Phys. **88**, 7739 (1988).
[30] W. H. Press, B. P. Flannery, S. A. Teukolsky, and W. T. Vetterling, *Numerical Recipes* (Cambridge, Cambridge, 1987); R. Fletcher, *Practical Methods of Optimization* (Wiley, New York, 1990).
[31] I. Prigogine, *From Being to Becoming* (Freeman, San Francisco, 1980).
[32] J. M. H. M. Scheutjens and G. J. Fleer, J. Phys. Chem. **83**, 1619 (1979); **84**, 178 (1980); O. A. Evers, J. M. H. M. Scheutjens, and G. J. Fleer, Macromolecules **23**, 5221 (1990); F. A. M. Leermakers and J. M. H. M. Scheutjens, J. Chem. Phys. **89**, 3264 (1988).
[33] GOLIAD software package for simulation of interfacial phenomena of chain molecules, Department of Physical and Colloid Chemistry, Wageningen Agricultural University, Dreijenplein 6, 6703 HB Wageningen, The Netherlands.
[34] P.-G. de Gennes, Riv. Nuovo Cimento **3**, 187 (1977) (reprinted in P.-G. de Gennes, *Series in Modern Matter Physics* (World Scientific, Singapore, 1992), Vol. 4.
[35] P.-G. de Gennes, *Scaling Concepts in Polymer Physics* (Cornell University, Ithaca, NY, 1979).
[36] M. Doi and S. F. Edwards, *The Theory of Polymer Dynamics* (Clarendon, Oxford, 1986).
[37] E. A. Dimarzio and R. J. Rubin, J. Chem. Phys. **55**, 4318 (1971).
[38] W. E. McMullen and K. F. Freed, J. Chem. Phys. **92**, 1413 (1990).
[39] H. E. Cook, Acta Metall. **18**, 297 (1970).
[40] Jan Scheutjens (personal communication).
[41] R. A. Horn and C. R. Johnson, *Matrix Analysis* (Cambridge University, Cambridge, 1992).
[42] T. L. Hill, *An Introduction to Statistical Thermodynamics*, 2nd ed. (Addison–Wesley, Reading, MA, 1962), Chaps. 20–21.
[43] J. Keizer, *Statistical Thermodynamics of Nonequilibrium Processes* (Springer, New York, 1987).
[44] D. Chandler, *Introduction to Modern Statistical Mechanics* (Oxford University, New York, 1987).
[45] H. Risken, *The Fokker–Planck Equation* (Springer, Berlin, 1989).
[46] C. W. Gardiner, *Handbook of Stochastic Methods* (Springer, Berlin, 1990).
[47] The software program dyn2d.f with which the numerical results were obtained is the property of Akzo. For more information, contact H. Dijkman, Department of Applied Mathematics, P.O. Box 9300, 6800 SB Arnhem, The Netherlands.